# AN OBJECTIVE, STATISTICAL SYSTEM FOR SHORT-TERM PROBABILISTIC FORECASTS OF CONVECTION

**Joby L. Hilliker**

Department of Geology and Astronomy
West Chester University
West Chester, Pennsylvania

**George S. Young and J. Michael Fritsch**

Department of Meteorology
The Pennsylvania State University
University Park, Pennsylvania

***Abstract***

*An objective statistical system that generates short-term probabilistic forecasts of convection (radar reflectivity ≥ 40 dBZ) solely from observational input is presented. This prototype is tested for Oklahoma City (OKC) by using several high-resolution regional datasets including 4-km resolution WSR-88D radar data, 404 MHz profiler data, and surface data from the Oklahoma mesonet. Data from the traditional, 12-h radiosonde network are also included. Antecedent observations (predictors) are correlated to future convection observations at OKC (the predictand). This procedure is repeated for 11 lead times between 6 and 360 min, inclusive, with each forecast equation containing 4-10 of the most powerful predictors.*

*Radar data provide the greatest contribution to skill, particularly for lead times ≤ 60 min. Specifically, the upstream percent areal coverage of reflectivities above a given threshold is the most powerful predictor of convection for all lead times. As lead times increase, an increasing contribution comes from the surface mesonet and then upper-air data. The absolute value of convergence and climatological departure of relative humidity are the most powerful predictors from the mesonet data. By 360 min, the final equations include a synergistic combination of predictors from radar, surface, and upper-air data.*

*The overall performance of the prototype system is encouraging. When applied to independent data, the system has a skill score of 0.39 relative to persistence climatology (alternatively, a 39% improvement in mean squared error) at 12-min lead times. Skill gradually decreases to 0.09 by the 360-min lead time, although significance testing reveals that forecast performance remains superior to persistence climatology at the 99.95% level.*

## 1. Introduction

Certain industries, such as aviation, require far more specific and frequent weather guidance than that provided by traditional synoptic-scale forecasts of one to three day lead times. For example, the efficiency of air-traffic flow is sensitive to local ceiling, visibility, and wind conditions that often differ substantially over distances and time periods not resolved by conventional synoptic guidance. Likewise, variations in the winds at cruising altitude can substantially affect fuel burn (Qualley 1997), while rapidly-changing convective storms can force unexpected and expensive diversions (Kulesa 2002). It is estimated that the effects of weather cost the airline industry over three billion dollars annually (Sankey et al. 2000).

The present study focuses on improving convection forecasts because thunderstorms are the most disruptive weather feature affecting aircraft operation within the United States (Post et al. 2002). The National Research Council (2003) has determined that thunderstorms are a factor in more than half (60%) of all weather-related delays. It is estimated that of the billions of dollars the airline industry expends each year due to weather, at least half can be attributed to thunderstorms (Evans 2000). Convection is also a safety concern, particularly for general aviation, with convection being the second leading cause of weather-related deaths and accidents (National Transportation Safety Board 1993).

### *a. Aviation industry needs*

These aforementioned statistics present compelling reasons for constructing thunderstorm forecasting products for the aviation industry. It is instructive, first, to provide insight into aviation operations, and their impact by adverse weather conditions. The reader is encouraged to review MacKeen et al. (1999) for detail on the impact of thunderstorms on daily operations. In doing so, a thunderstorm forecasting system possessing the following qualities would be of greatest utility to the aviation industry:

- *short-term lead times:* capable of outputting forecasts for lead times <6 h,
- *frequently-updating:* updates forecasts in a few minutes,
- *quantifies risk*: provides measures of uncertainty (i.e., reliable probabilities) of convection occurrence,
- *objective*: uninfluenced by human forecasting bias or emotion,
- *gridded*: generates forecasts for a domain, and
- *fine spatial-resolution*: discerns hazardous conditions on the meso-gamma (2-20 km) scale.

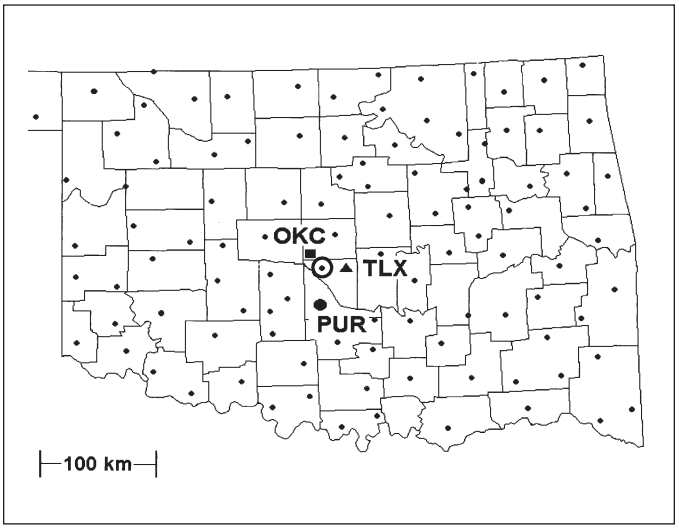


**Figure 1a.** Observation sites considered in the study. The thunderstorm forecast system is developed for Oklahoma City, OK (OKC) (square). Radar data are from the WSR-88D radar site at Twin Lakes, OK (TLX) (triangle). Profiler data are from Purcell, Oklahoma (PUR) (larger, black circle). Smaller gray circles are surface reporting sites comprising the Oklahoma mesonetwork. The closest mesonet site to OKC is Norman, Oklahoma, circled in the middle of the map.

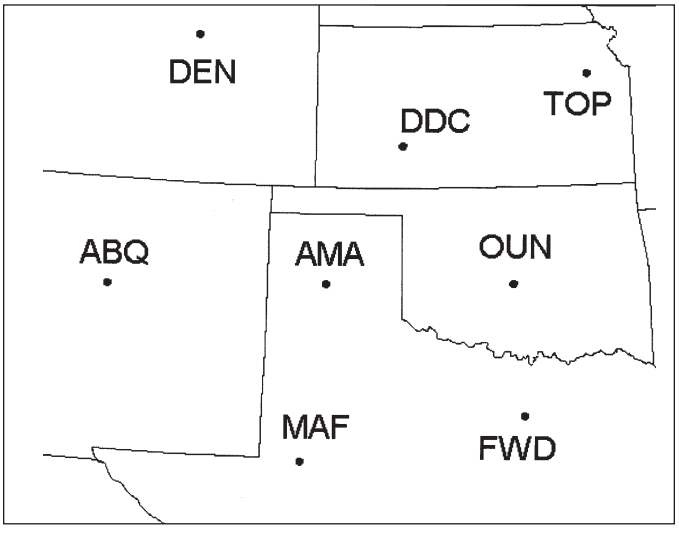


**Figure 1b.** Radiosonde sites considered in the study: Denver, Colorado (DEN); Dodge City, Kansas (DDC); Topeka, Kansas (TOP); Norman, Oklahoma (OUN); Fort Worth, Texas (FWD); Midland, Texas (MAF); Amarillo, Texas (AMA); and Albuquerque, New Mexico (ABQ).

The first two qualities are necessary because convective situations can rapidly change during the short duration of a domestic flight. As a result, air-traffic management continually makes short-term decisions. In fact, Forman et al. (1999) revealed that the optimal lead time needed to manage air traffic within 80 km of an airport (i.e., terminal traffic) is 30 min.

Moreover, the decision-driven traffic flow system is deterministic, meaning that a single forecast is produced for each lead time. Considering the multitude of non-linearities that interact in the atmosphere, the approximations essential to numerical model initialization, and the various parameterization schemes necessary to run a numerical model, it is not surprising that there can be large uncertainty (and bias) in model forecasts. There has been increasing effort by traffic flow management to account for this inherent uncertainty through cost-benefit decision-making – all in an effort to operate at peak efficiency and minimize the airlines' operating costs (Keith and Leyton 2004). This suggests that statistical techniques that provide objective, quantitative measures of uncertainty (i.e., reliable probabilities) would also be of value.

The last two qualities emphasize the spatial properties of the forecast output. A product that generates forecasts over a domain could warn of enroute hazardous conditions. Furthermore, a product with high spatial resolution can account for possible convection in the departure/arrival zones surrounding airports. There is a risk, however, that such output can lose its utility if the spatial resolution becomes too fine. Because convection is a rare event, the forecast probabilities may become too low to be meaningful (K. K. Hughes, personal communication 2006).

*b. Evolution of the "obs-based" system*

Numerous techniques have been developed to begin to satisfy the above requirements for short-term forecasting of convection, and Wilson et al. (1998) provides a historical perspective. In the past decade, the *Terminal Convective Weather Forecast* (TCWF), after Theriault et al. (2000); the *Collaborative Convective Forecast Product* (CCFP), after Seseske and Hart (2006); and the *National Convective Weather Forecast* (NCWF) System, after Megenhardt et al. (2000) have been created. Other successful products include the *Auto-Nowcast Environment*, after Mueller et al. (2000); the Rapid Update Cycle (RUC), after Benjamin et al. (2004); and the *Convective Probability Forecast* (CPF) Product which outputs probabilities with lead times ≥ 2 h., after Weygandt and Benjamin (2004).

Most relevant to the present study are statistical products that generate probabilities for a gridded domain using a history of observations. Using a Model Output Statistics (MOS) approach (Glahn and Lowry 1972), Charba (1979) developed equations to forecast probabilities of severe thunderstorms across the United States 2-6 h in advance for an array of boxes 155 km on a side. More recently, Kitzmiller et al. (2002) developed a 0-3 h gridded lightning forecast product, updated hourly, for 40 km on a side. A similar product, with a finer 20-km resolution, was developed by Hughes (2004).

The purpose of the present work is to demonstrate a new system ("obs-based system," hereafter) that may also provide utility to the aviation industry because it possesses the aforementioned qualities. One approach in creating a system with these properties is to extend the obs-based system of Vislocky and Fritsch (1997; hereafter VF97) to a gridded array of points for convection prediction. Additionally, incorporating multiple data types in the derivation of statistical forecast equations would further extend the system. Hilliker and Fritsch (1999; hereafter HF99) and Grover (2002) had shown that including

additional data types (upper-air and radar data, respectively) increased forecast accuracy when compared to forecasts generated solely from surface observations. Furthermore, since Leyton and Fritsch (2003, 2004) demonstrated improved accuracy of obs-based techniques by utilizing high-frequency observations, convection forecasts should be constructed with increased temporal and spatial resolution.

This study incorporates radar data of 4-km resolution, thus allowing forecasts to be outputted at the same resolution (i.e., gridded boxes are 4 km on a side). This fine resolution is particularly appealing since convective activity may be resolved within critical approach and departure zones. Moreover, since the radar data has a 6-min temporal frequency[1], output could be updated at this ultra-short-term frequency and focus on a spectrum of lead times ranging from 6 to 360 min. A suite of lead times would allow a variety of users in the aviation industry to utilize this guidance regardless of their area of responsibility. For example, knowledge that convection will approach in 30 min is useful for outdoor baggage transporters or personnel who monitor terminal traffic during a convective period (D'Arcangelo, personal communication 2002; Forman et al. 1999). On the other hand, 4-h forecasts are ideal for dispatchers who determine optimal air routes and estimate the needed fuel for each flight (Hubright, personal communication 2002).

Descriptions of the datasets used as input into the forecast system and their preprocessing are detailed in Section 2. The statistical design of the system is documented in Section 3. Results from predictor testing on a dependent data set are presented in Section 4, while quantitative measures of skill of the forecast system based on independent samples are shown in Section 5. A summary of results and concluding remarks are provided in Section 6.

## 2. Data

The region centered on the Oklahoma City airport (OKC; Fig. 1a) was selected for developing and testing the prototype convection forecasting system. This region provides a unique and extensive array of observing platforms suitable for product development that satisfies the aviation industry's short-term forecasting requirements. The following, mainly high-resolution, datasets were compiled for four May-June periods from 1995 to 1998. The May-June period was chosen since it corresponds to the climatological peak frequency of convection in Oklahoma (Williams 1994).

### *a. Radar data*

NEXRAD Information Dissemination Service (NIDS) provided Level III, high resolution (4-km) composite reflectivity radar data. Composite radar data is the maximum reflectivity over a given area using the various scan angles (Weather Services Incorporated 2007). This data serves as both input and verification in this study. Over 40,000 radar images were obtained for the Twin Lakes, Oklahoma (TLX) radar site, located ~30 km east-southeast of OKC (Fig. 1a).

Composite radar data may be more desirable than base reflectivity radar data for aviation purposes because hazardous weather may be occurring above and/or below the particular elevation tilt used to create the base reflectivity. However, a forecast system utilizing composite radar data may lead to over-warning of forecasts if base reflectivity data is used as verification (i.e., the observed/actual reflectivity).

### *b. Wind profiler data*

The National Oceanic and Atmospheric (NOAA) Profiler Network (NOAA 2007) was the source for the 404 MHz wind profiler data obtained from the Purcell, Oklahoma site. (Fig. 1a). Wind direction and speed for every 250 m, up to 16,250 m, were available at the top of each hour.

### *c. Surface data*

Surface data came from the Oklahoma Mesonetwork (Brock et al. 1995). All 114 sites across Oklahoma, with an average 30-km horizontal spacing between sites, were contained in the database (Fig. 1a). Observations, available every 5 min, included 10-m wind direction and speed, 1.5-m temperature, relative humidity (RH), solar radiation, rainfall, and pressure data.

### *d. Radiosonde data*

Radiosonde data (every 12 h) for Norman (OUN), Oklahoma and seven other sites surrounding OUN (Fig. 1b) came from NOAA/National Weather Service (NWS) (NOAA/OAR 2007).

When constructing a forecast system based on observations, it is critical to obtain the highest quality datasets. Degraded databases dull statistical signals or even generate false signals. This, in turn, degrades the performance of the forecast equations and results in an inferior forecast system. Extensive efforts were employed to quality control the high-resolution datasets. Summaries of the experiments leading to quality control technique development and the techniques' performance are presented in Hilliker (2002).

## 3. Methodology: Statistical Design of Forecasting System

Designing the forecasting system requires defining the predictand (i.e., forecast variable), choosing appropriate lead times, and selecting predictors that are likely to be of value for forecasting convection.

### *a. The predictand*

For this study, "convection" is defined as a radar pixel with composite reflectivity value ≥40 dBZ (decibels). This corresponds approximately to a Video Integrated

[1]The temporal frequency of WSR-88D radar data can be increased to ~4 min by using VCP 12 (Lee 2004).

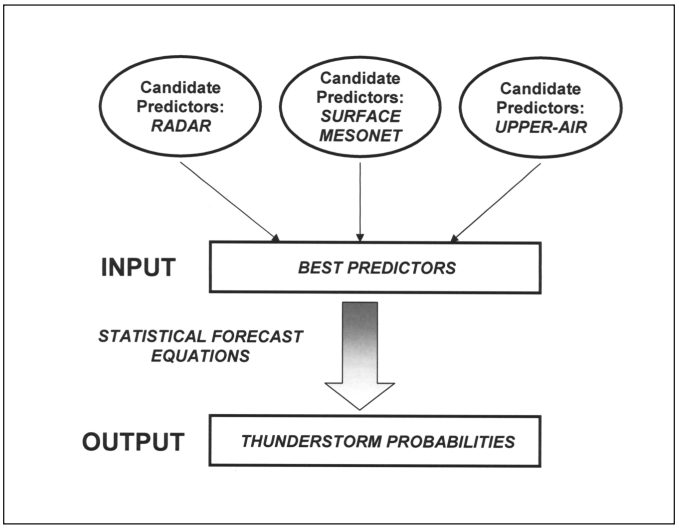


**Figure 2.** Schematic of the convection forecasting system. The most powerful predictors from candidate sets of radar, surface mesonet, and upper-air predictors are linked by using statistical model fits to form forecast equations for each lead time. Predictor values are inputted into the equations, which allow thunderstorm probabilities to be generated.

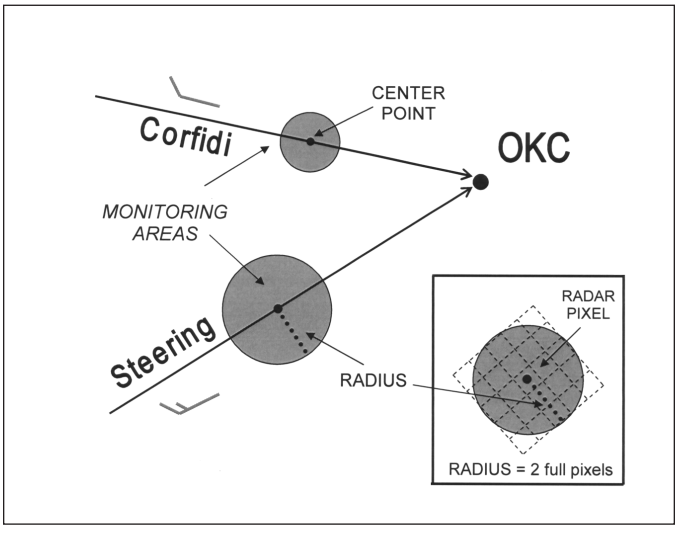


**Figure 3.** Schematic of the "monitoring area" concept. A monitoring area (gray circle) is an array of radar pixels upstream from OKC used to monitor approaching convection. For each lead time, two monitoring areas are constructed – one using the steering vector, the other using the Corfidi vector. The center of each monitoring area ("center point") is calculated based on the direction and magnitude of the particular vector as well as lead time. Inset shows an array of radar pixels with a radius of two full pixels.

Processor (VIP) level 3 and is traditionally the intensity that pilots begin to avoid by asking for deviations (Rhoda et al. 2000). Other thunderstorm forecasting studies (Mahoney et al. 2000; Theriault et al. 2000) have also used a threshold of 40 dBZ for defining convection in radar data.

Forecasts of convection occurrence (the predictand) are made for the radar pixel containing OKC. *For the OKC pixel*, an "event" is defined as the presence of convection in a given radar image. With respect to model development, the predictand in this study is necessarily binary, with events (non-events) coded as "1" ("0").

**Table 1.** Suite of forecast lead time (in minutes) tested in the study. Also shown are the temporal windows applied for each lead time and number of radar images falling within that window.

| Lead Time (Min) | Temporal Window (Min) | Mode Number of Sweeps in Window |
|---|---|---|
| 6 | 5-6 | 1 |
| 12 | 11-13 | 1 |
| 18 | 17-19 | 1 |
| 24 | 22-26 | 1 |
| 30 | 28-32 | 1 |
| 45 | 42-48 | 1 |
| 60 | 55-65 | 2 |
| 90 | 84-96 | 2 |
| 120 | 110-130 | 4 |
| 240 | 220-260 | 7 |
| 360 | 330-390 | 15 |

Because convection is a rare event (average hourly frequency of 1.3% at OKC), "regionalization" was employed. Here, data from additional sites with comparable climates were included to increase the number of events, thereby strengthening the statistical signal. In this study, the eight pixels surrounding the OKC pixel were included in the development of a single forecast equation.

As a result of expanding the database to include multiple pixels, additional terminology is needed. Each radar image is defined as a separate "case" for each pixel. Therefore, one radar image produces nine cases, corresponding to each of the nine pixels. For example, if convection was present in two pixels in each of three successive radar images, 27 (3 images x 9 pixels) cases would result, of which six (3 images x 2 pixels) would be events.

### *b. Lead times*

Table 1 shows the 11 forecast lead times; they range from 6 min to 6 h. Because these times are single, transient moments in the future, a temporal flexibility ("window") of +/- 8%[2] of the lead time was applied to extract a stronger statistical signal. As an example, an event verified for the 4-h lead time if convection was observed in *any* radar image in the period defined by 3 h 40 min to 4 h 20 min in the future.

[2] The choice of +/-8% stems from applying reasonable windows of +/- 5 min at the 60-min lead time, increasing to +/- 30 min at the 360-min lead time.

**Table 2.** Properties of the pre-selected (stationary) monitoring boxes as a function of lead time. The second column indicates the length (in km) of the box. Subsequent columns list the location of the center with respect to OKC of the suite of eight stationary boxes prescribed in the study. Centers of the eight boxes are located in each of the eight primary compass directions away from OKC. For example, (-4,8) under "NW" indicates that the center of the northwestern box is 4 km west and 8 km north of OKC.

| Lead Time (Min) | Box Length (KM) | LOCATION OF CENTER OF BOX WITH RESPECT TO OKC (ΔX, ΔY) (KM) | | | | | | | |
|---|---|---|---|---|---|---|---|---|---|
| | | W | NW | N | NE | E | SE | S | SW |
| 6 | 12 | (-4,0) | (-4,8) | (0,8) | (4,8) | (4,0) | (4,-8) | (0,-8) | (-4,-8) |
| 12 | 12 | (-8,0) | (-8,8) | (0,8) | (8,8) | (8,0) | (8,-8) | (0,-8) | (-8,-8) |
| 18 | 16 | (-12,0) | (-12,16) | (0,16) | (12,16) | (12,0) | (12,-16) | (0,-16) | (-12,-16) |
| 24 | 16 | (-16,0) | (-16,16) | (0,16) | (16,16) | (16,0) | (16,-16) | (0,-16) | (-16,-16) |
| 30 | 24 | (-20,0) | (-20,24) | (0,24) | (20,24) | (20,0) | (20,-24) | (0,-24) | (-20,-24) |
| 45 | 40 | (-28,0) | (-28,40) | (0,40) | (28,40) | (28,0) | (28,-40) | (0,-40) | (-28,-40) |
| 60 | 56 | (-40,-4) | (-40,52) | (0,52) | (40,52) | (40,-4) | (40,-60) | (0,-60) | (-40,-60) |
| 90 | 72 | (-40,-4) | (-40,68) | (0,68) | (40,68) | (40,-4) | (40,-68) | (0,-68) | (-40,-68) |
| 120 | 88 | (-48,-8) | (-48,96) | (0,96) | (48,96) | (48,-8) | (48,-100) | (0,-100) | (-48,-100) |
| 240 | 120 | (-64,-8) | (-64,112) | (0,112) | (64,112) | (64,-8) | (64,-128) | (0,-128) | (-64,-128) |
| 360 | 160 | (-84,-12) | (-84,148) | (0,148) | (84,148) | (84,-12) | (84,-148) | (0,-148) | (-84,-148) |

*c. Obtaining predictors*

Figure 2 shows a blueprint of the obs-based system. The most powerful (i.e., significant) predictors from the radar, mesonet, and radiosonde datasets are linked with a statistical model to form a forecast equation valid for a given lead time. The ultimate success of this system depends upon the robustness of the predictors included in the final equations. Since a limitless number of combinations of variables can be created, physical reasoning was used in devising a more manageable number ("pool") of candidate predictors. This is where knowledge of thunderstorm dynamics, and the ambient conditions that produce, sustain, and weaken them, is critical in guiding the builder of a predictive system.

The following subsections summarize the selection of various predictors and the strategies implemented in obtaining them. A more extensive discussion on methodology, including an exhaustive review of candidate and final predictors, can be found in Hilliker (2002).

1) Radar predictors

One strategy in identifying potentially skillful predictors from radar data is based on the premise that a particular wind direction dictates thunderstorm movement. A widely-recognized vector that specifies movement of individual thunderstorms is the mean flow in the cloud layer ("steering vector," hereafter), often calculated as a vector average of the 300-, 500-, 700-, and 850-mb winds (Fankhauser 1964). Consequently, mean cloud-layer flow is utilized in aspects of several thunderstorm forecast products (Theriault et al. 2000; Megenhardt et al. 2000; Mueller et al. 2000, 2003). For large convective systems (e.g., squall lines, mesoscale convective complexes), Corfidi et al. (1996) found that the vector difference between the low-level jet and the mean cloud-layer flow had a relatively high correlation (0.78-0.80) to a system's movement. Therefore, both the steering and Corfidi vectors were examined as potential predictors.

Profiler data from Purcell, OK, were used to compute the steering and Corfidi vectors. Vectors were calculated at the top of each hour and interpolated within the hour to correspond with the 6-min time stamps of the radar images. The 850-mb flow was used as a proxy for the low-level jet in computing the Corfidi vector.

Once the steering and Corfidi vectors were known, areas were defined upstream from OKC as a means to gauge, or monitor, approaching convection. Figure 3 illustrates this concept. The centers of these monitoring areas (hereafter "center points") can be located based on each vector's magnitude and direction. Note there would be 22 monitoring areas for each radar image - two vectors for each of the 11 lead times.

Figure 3 shows center points and monitoring areas for a 30-min lead time. If the steering flow were 245° at 15 m $s^{-1}$ in this example, the center point would be (15 m $s^{-1}$) (1800 s) = 27 km southwest of OKC. Naturally, the center points would be farther upstream for longer lead times. The same methodology was then repeated using the Corfidi vector.

Given the location of an upstream monitoring area, it was then necessary to determine the optimal size of the monitoring area for each lead time. To accomplish this, various-sized arrays of pixels were constructed in a pilot study to determine the optimal size. Each array approximated a circle, with the center pixel of each array co-located with the center point. As an example, the inset in Fig. 3 depicts a circle of radius of two full pixels.

**Table 3.** Selected candidate radar predictors, and their notation.

| CANDIDATE RADAR PREDICTOR | NOTATION |
|---|---|
| Reflectivity at OKC | **R** |
| Percent areal coverage of reflectivity within stationary monitoring boxes (located in direction, d) from OKC | $^{d}$**B** |
| Percent areal coverage of reflectivity within upstream monitoring areas. Location of upstream area determined by using the steering flow | **S** |
| Same as above, but by using the Corfidi vector | **C** |
| Same as **S** and **C**, but the value of the "percent areal coverage" itself dictates whether the steering or Corfidi vector is used | **P** |
| Same as **S** and **C**, but the value of the "interconnectedness" dictates whether the steering or Corfidi vector is used | **I** |
| Temporal changes of the predictors above | Predictor preceded by "Δ" (e.g., Δ**S**) |

**Table 4.** Selected candidate surface mesonet predictors.

| CANDIDATE MESONET PREDICTOR |
|---|
| Temperature (°C) |
| Relative Humidity (%) |
| Dewpoint (°C) |
| Relative Humidity Difference (%) (Spatial) |
| Dewpoint Difference (°C) (Spatial) |
| Climatological Departures on all of the above parameters |
| Convergence (m s$^{-1}$) |
| Absolute Value of Convergence (m s$^{-1}$) |
| Binary Logic Predictors (BLP) |

A suite of 36-sized circles was empirically tested, ranging from a radius of zero (i.e., the center pixel itself) to 140 pixels. For each array for each lead time, a "percent coverage" (**P**) was computed – a parameter defined as the fraction of radar pixels inside the circle of a given threshold value to the total number of pixels comprising the circle (Germann and Zawadski 2002).

**Table 5.** Selected candidate upper-air predictors. Notation (second column) adheres to the following convention: $_{p}\mathbf{X}_{ABC}$, where "p" is the pressure level of the parameter (where applicable), and "ABC" is the radiosonde identifier, from Fig. 1b.

| CANDIDATE UPPER-AIR PREDICTOR | NOTATION |
|---|---|
| Lifted Condensation Level (mb) | $\mathbf{LCL}_{ABC}$ |
| Convective Available Potential Energy (J kg$^{-1}$) | $\mathbf{CAPE}_{ABC}$ |
| Lapse Rate (700-500 mb) (°C) | $\mathbf{LR}_{ABC}$ |
| Total Totals (°C) | $\mathbf{TT}_{ABC}$ |
| K-index (°C) | $\mathbf{K}_{ABC}$ |
| Lifted Index (°C) | $\mathbf{LI}_{ABC}$ |
| 800-700 mb Mean Relative Humidity (%) | $\mathbf{RH87}_{ABC}$ |
| 700-500 mb Mean Relative Humidity (%) | $\mathbf{RH75}_{ABC}$ |
| 800-500 mb Mean Relative Humidity (%) | $\mathbf{RH85}_{ABC}$ |
| 500 mb Relative Vorticity (m s$^{-1}$) | **V** |
| Temperature (at pressure, p) (°C) | $_{p}\mathbf{T}_{ABC}$ |
| Relative Humidity (at pressure, p) (%) | $_{p}\mathbf{RH}_{ABC}$ |
| Climatological Departure of Relative Humidity (at pressure, p) (%) | $_{p}\mathbf{RH}'_{ABC}$ |

In addition, because the forecasting system must deal with both individual thunderstorms and organized convective systems, a procedure was developed that "chooses" the appropriate vector based on the spatial properties of the convection. This required the forecast system to be able to distinguish between events composed predominantly of individual thunderstorms and those that exhibited a larger, contiguous area of convection.

To achieve this, two parameters were defined to characterize the spatial scale of the convection: a) percent coverage (**P**), defined earlier; and b) "interconnectedness" (**I**) or number of pixels ≥ 40 dBZ connected to (i.e., "touching," or having a common side to) another ≥ 40 dBZ pixel within the monitoring area. Here, small (large) values of **P** or **I** correspond to smaller- (larger-) scale events.

To complement the monitoring areas, an additional set of pre-selected, or stationary, monitoring boxes (squares) was constructed, where **P** values were again computed. For each lead time, eight boxes were constructed, with centers located in each of the eight primary compass directions away from OKC. Table 2 shows the "box length" (i.e., the square's side distance) and placement with respect to OKC of each box as a function of lead time. Using a methodology similar to Grover (2002), monitoring boxes expand with lead time as their centers become more distant from OKC.

Naturally, the preceding predictors are relevant for convection already in progress. To forecast the development and dissipation of convection, temporal changes in percent coverage values were tested. Supplemental predictors, deemed most valuable for ultra-short-term lead times, included present and temporal changes in reflectivity at OKC. An abridged version of the candidate radar predictors tested is shown in Table 3.

2) Surface mesonet predictors

Table 4 shows an abridged list of surface mesonet candidate predictors. Example predictors include relative humidity, its departure from sample climatological values, and the spatial difference in dew-point between OKC and each of a 48 equally-spaced sample of mesonet sites, shown in Fig. 4.

Several studies (e.g., Byers and Braham 1949; Garstang and Cooper 1981) have shown the importance of boundary-layer convergence in thunderstorm evolution. Thus, derived parameters, such as surface convergence, and its absolute value (i.e., convergence or divergence) were also considered. Convergence values were computed using the line integral method (Zamora et al. 1987; Davies-Jones 1993), and diagnosed using various spatial resolutions by varying the number of mesonet sites included.

Another category of predictors, termed "binary logical predictors" (BLP, hereafter) was devised to identify areas that are traditionally associated with convective development (e.g., vicinity of cold fronts, dry lines). A BLP was assigned a value of "1" if three constructed parameters exceeded given thresholds; otherwise, the predictor was assigned a value of "0." One example BLP was "1" if:

a) the dewpoint at Norman, Oklahoma (*NORM*; circled in Fig. 1a), the closest mesonet site to OKC, were ≥20°C, and

b) the climatological departure of dewpoint at *NORM* were ≥4°C than that of *TEST*, a dummy mesonet site representing one of the 48 sample mesonet sites, and

c) the absolute difference in wind direction between *NORM* and *TEST* were ≥30°.

3) Upper-air predictors

Previous studies have shown the value of upper-air variables in short-term thunderstorm forecasting [e.g., relative humidity (Sanders and Garrett 1975); Total-totals index (Miller 1967)]. In addition to offering raw parameters observed at the eight radiosonde sites shown in Fig. 1b, each parameter's departures from the dataset's sample climatology were also considered. Kinematical variables, such as convergence and vorticity, were also tested for possible predictive value. Additional candidate upper-air predictors are shown in Table 5.

*d. Testing on the dependent data set*

Three years of the 4-yr database served as the dependent data set, from which the candidate predictors above were tested. The remaining year served as the independent data set, to which the forecast equations were applied and probabilistic thunderstorm forecasts were generated. To ensure that the most robust statistical results were obtained, "cross-validation" was applied. In cross-validation, the 4-yr database was subdivided into four combinations of larger (3-yr) dependent data sets and smaller (1-yr) independent datasets.

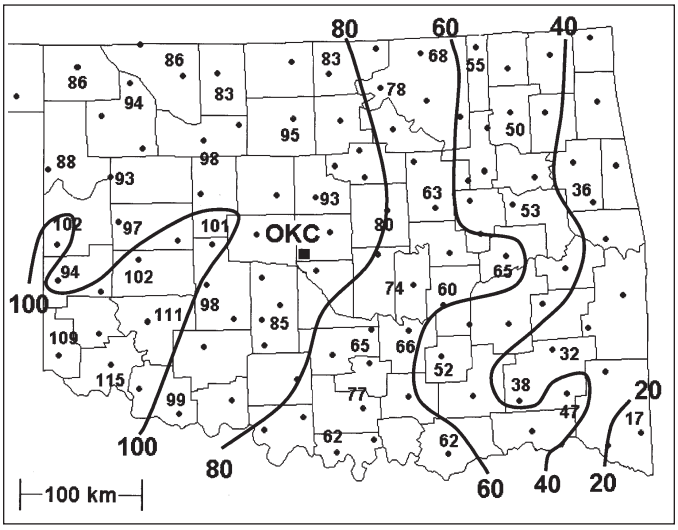


**Figure 4.** Contours of t-values, using a sample of 48 mesonet sites, of the climatological departure of relative humidity as a predictor for 240-min convection forecasts.

The statistical software package *IMSL* ascertained the most powerful predictors, their t-values, ranking order, as well as explained variances (Visual Numerics, Inc. 1997). The t-value measures the predictor's degree of linear association with thunderstorm occurrence, with higher absolute values indicating stronger association.

To obtain an optimal set of predictors, the "efroymson" method was selected as the stepwise regression procedure. This method is similar to a forward selection procedure in that a predictor is chosen based on its ability to independently produce the largest reduction in the residual sum of squares. However, when a new predictor is added to the subset, the efroymson method determines if any of the previously selected predictors in the subset no longer contributes significantly to the modeled fit. If this is the case, the predictor is eliminated.

In addition, the number of predictors included in the final equations depends on a prescribed "cutoff" t-value ($t_c$). Once the absolute value of the t-value of the next significant predictor falls below $t_c$, no additional predictors are included, and the equation is finalized. Although it may be tempting to include many predictors to achieve the best modeled fit, the risk of "overfitting" increases. Over fitting is defined as the inclusion of predictors only meaningful to the dependent data set, which results in degraded equation performance when applied to a different, or independent, set of data.

To objectively optimize $t_c$, one of the 3-yr dependent data sets was sacrificed by subdividing it into a 2-yr

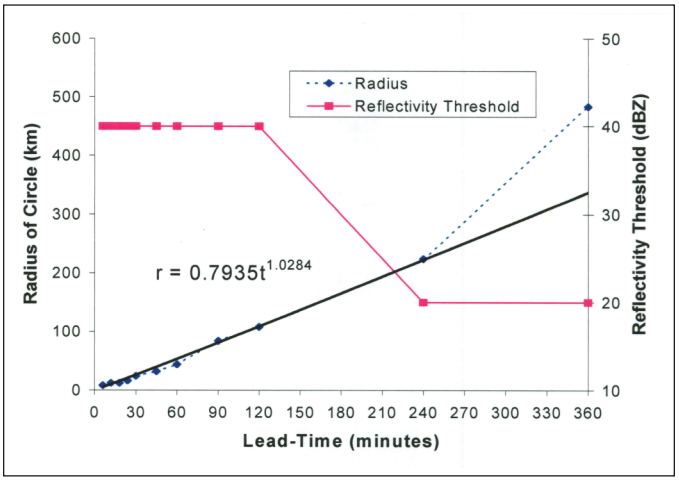


**Figure 5.** Optimal radius (in km) of monitoring area (dashed blue line) as a function of lead time using the steering vector. The bold line indicates a best fit using the labeled power equation. Also shown is the optimal reflectivity threshold (solid red line) for computing percent coverages.

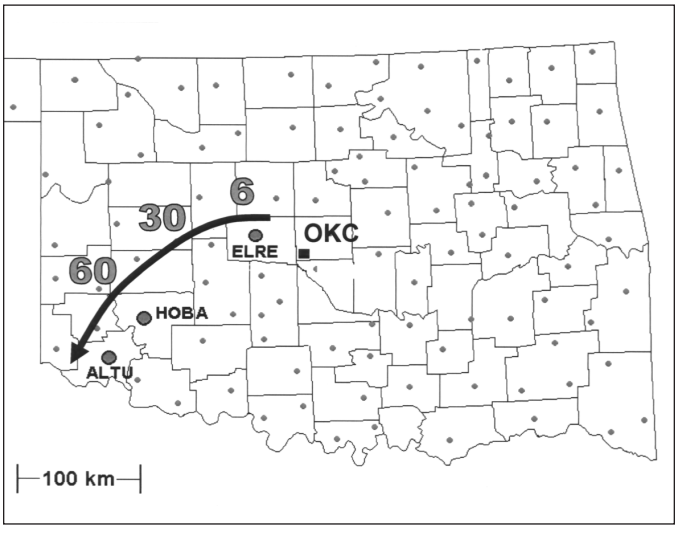


**Figure 6.** Location of the most beneficial surface mesonet sites (larger gray circles) for thunderstorm forecasting — using RH' as a predictor — as a function of lead time (in minutes, and labeled next to the relevant station). "ELRE" is El Reno, "HOBA" is Hobart, and "ATLU" is Altus.

sub-dependent set and a 1-yr sub-independent set. Using the sub-dependent data, a suite of forecast equations was then developed by varying the number of predictors, dictated by testing various $t_c$ values. Each equation was then applied to the sub-independent data to generate forecast probabilities. The mean squared errors (MSE) between these probabilities and the observed were then calculated to estimate the optimal $t_c$ for each lead time. In this study, a $t_c$ of 20 minimized the MSE for lead times ≤ 60 min; by the 360-min lead time, $t_c$ increased to 90. In general, this allowed 4-10 predictors to be included in the final equations.

Additional information on stepwise regression, choosing t-values, and overfitting can be found in Wilks (1995) and Neter et al. (1996).

## 4. Results: Dependent Data Set

An examination of how each of the data types was utilized in the forecasting system is presented. Results presented here are based upon the dependent data set consisting of 1995, 1996, and 1998 data, which comprised ~200,000 cases and ~6800 events. No significant departures in the nature of the best predictors were noted for the other dependent data sets.

### *a. Radar predictors*

Results indicated that through a 45-min lead time over all cases in the database, the steering vector was more highly correlated to the predictand (thunderstorm occurrence) than the Corfidi vector. After 45 min, there was no significant favorite; however, each vector often provided valuable statistically independent information.

Figure 5 shows the highest correlated monitoring area radius at which to extract percent coverages using solely the steering vector. This analysis revealed that the best radius increased from 8 km for a 6-min lead time to 492 km for a 360-min lead time. The superimposed bold line is a best linear fit of radius to lead time using a power equation. Because the coefficient and exponent in the equation are both close to unity, the optimal radius (in km) is nearly equal to the lead time (in min).

Figure 5 also reveals the optimal reflectivity threshold for thunderstorm forecasting as a function of lead time. For lead times ≤ 240 min, a 40 dBZ reflectivity threshold (the same threshold as the predictand) was preferred for computing percent coverages. For longer lead times, the optimal threshold decreased to 20 dBZ.

### *b. Surface mesonet predictors*

When solely mesonet data were offered to the predictor selection routine, the departure of relative humidity from climatology (RH′) was consistently chosen as a powerful predictor. Another frequently appearing predictor was convergence, an anticipated result since it is well known that low-level convergence in a conditionally unstable atmosphere is an excellent predictor of convection. In this study, however, the *absolute* value of the convergence was generally a better predictor than convergence alone. It is hypothesized that this parameter is indicative of disturbed conditions reflecting the convergence/divergence dipole signature that typically occurs with the passage of a thunderstorm.

In addition to ascertaining useful parameters, it was also enlightening to determine *where* the most influential mesonet sites are located. Figure 4 shows contours of t-values of RH′ using a 48-station sample for a 240-min forecast of convection. Note the maximum is across southwest Oklahoma, with Altus (*ALTU* in Fig. 6) the most significant mesonet site. In this example, southwest Oklahoma is a region of *positive* t-values, indicative of a positive association between RH′ and convection occurrence (i.e., the greater the station's RH is above its climatology, the greater the chance of storms at OKC in 240 min). The second and third most powerful stations for RH′ for the 240-min lead time (not shown) are located in

the Oklahoma panhandle and north-central Oklahoma, respectively. Note these sites do not come from the region of maximum t-values; rather, they are chosen because they come from regions that provide statistically independent information to the forecast. One possibility why RH′ was chosen in vastly different areas was to optimize the system's ability to "detect" if, and where, a triggering mechanism for convection (e.g., the dry line) exists.

Plots similar to Fig. 4 were constructed for each lead time. As a summary, Fig. 6 shows the locations of the most significant mesonet sites for select lead times using RH′ as a predictor. As expected, the most significant site progresses farther to the west, and then southwest, with lead time. For lead times ≥ 60 min, *ALTU* – the farthest station in southwest Oklahoma – is chosen. It is likely that sites in northwest Texas would have been chosen for longer lead times if such data were available.

*c. Upper-air predictors*

Results from the predictor screening indicated no upper-air parameters present in the top 20 final predictors for lead times ≤ 30 min. However, the number and significance of upper-air predictors increased with lead time, with four upper-air predictors present for the 60-min lead time. By 360-min, eight were included in the top 20 final predictors. The majority of these predictors focused on atmospheric stability and amount of mid-tropospheric (400 mb) moisture. As expected, the majority of predictors were for Norman, although data from surrounding upper-air stations (e.g., CAPE at Midland, Texas; Lifted Index at Dodge City, Kansas) provided additional independent information.

*d. Final set of predictors*

The complete forecast equations include an optimal blend of predictors from all three data types. The top five predictors (in order of significance) for each lead time using the 1995, 1996, and 1998 dependent data set are shown in Fig. 7. Although there were slight variations in the nature and order of predictors from the other combinations of dependent data sets, the predictors are an excellent representation of the most powerful for short-term forecasts of thunderstorms.

Several observations on the nature of the final set of predictors can be made. Foremost, the upstream areal percent coverage of high reflectivities is the most frequently included predictor for all lead times. Note that both the stationary boxes (**B** in Fig. 7) and those areas that incorporate the upper-level wind flow (**S** and **C**) populate the final set. Specifically, the most powerful predictor for lead times ≤ 45 min is $^{W}\mathbf{B}$, the areal coverage of reflectivity ≥ 40 dBZ west of OKC, an intuitive result. Note that this predictor ranks ahead of **R**, the most recent reflectivity observation at OKC, at the 6-min lead time. This signals an important departure from VF97, HF99, Leyton (2003), and Fritsch (2004) in that the most recent predictand observation is *not* the best predictor for the shortest allowable lead time given the temporal frequency of the observations.

Other top predictors included those that assessed the percent areal coverage (**P**) and interconnectedness (**I**) of the ongoing convection. Their popularity is encouraging in that the use of stratification techniques, albeit simple in this study, provided additional information. Finally, temporal changes in the above predictors occasionally appeared. For example, the 6-min change in reflectivity at OKC ($\Delta\mathbf{R}$) ranked third at the 6-min lead time, reveal-

| LEAD TIME (MIN) | PREDICTOR ORDER 1 | 2 | 3 | 4 | 5 |
|---|---|---|---|---|---|
| 6 | $^{W}$B | P | ΔR | R | ΔS |
| 12 | P | $^{W}$B | ΔS | I | S |
| 18 | $^{W}$B | P | ΔS | I | S |
| 24 | $^{W}$B | S | ΔS | I | P |
| 30 | $^{W}$B | S | ΔS | I | ΔS |
| 45 | $^{W}$B | ΔS | $^{NW}$B | ΔS | P |
| 60 | I | ΔS | $^{W}$B | BLP | P |
| 90 | S | BLP | C | ΔS | S |
| 120 | P | ΔS | BLP | $^{NW}$B | $^{NE}$B |
| 240 | S | BLP | ΔC | $_{400}$RH$_{OUN}$ | ΔC |
| 360 | P | BLP | $_{400}$RH$_{OUN}$ | LCL$_{OUN}$ | $^{S}$B |

LEGEND: Radar Predictor; Most Recent OKC Reflectivity Observation; Mesonet Predictor; Upper-air Predictor

**Figure 7.** Top 5 predictors (in order of significance) for short-term convection forecasting as a function of lead time. Predictor notation is referenced in Tables 3 & 5. Boxes are shaded with respect to data type, as shown in legend. "BLP" refers to constructed binary logic predictors by using the surface mesonet.

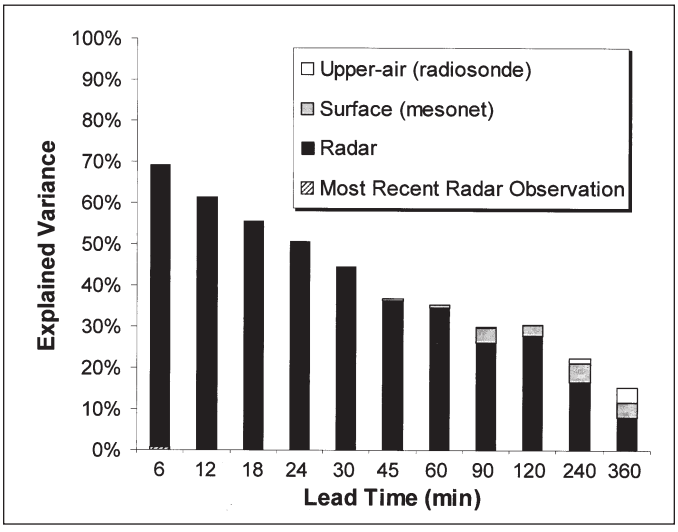


**Figure 8.** Explained variance (i.e., $R^2$ value) of observations-based forecasts as a function of lead time. The contribution of the explained variance from each of the data types is also shown. Radar contribution is shown in black, surface mesonet in gray, and upper-air in white. The independent contribution of the current radar observation at OKC for the 6-min forecast is denoted as cross-hatching.

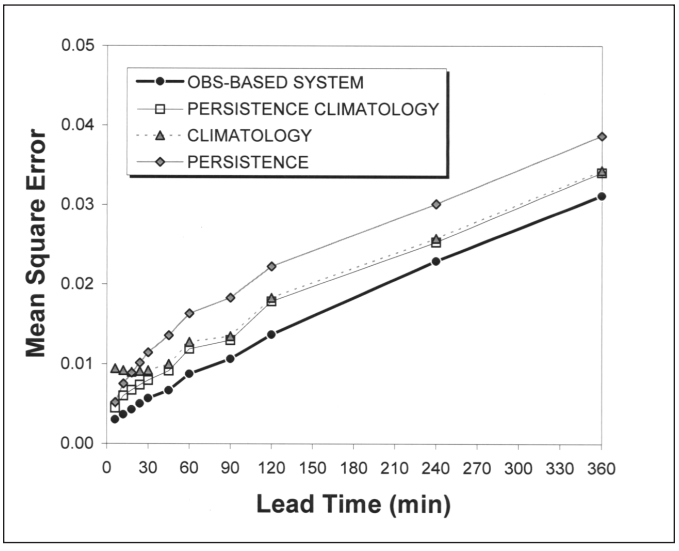


**Figure 9.** Mean square errors of the observations-based system (black line with circles), persistence climatology (solid gray line with squares), climatology (dashed gray line with triangles), and persistence (solid gray line with diamonds) as a function of lead time.

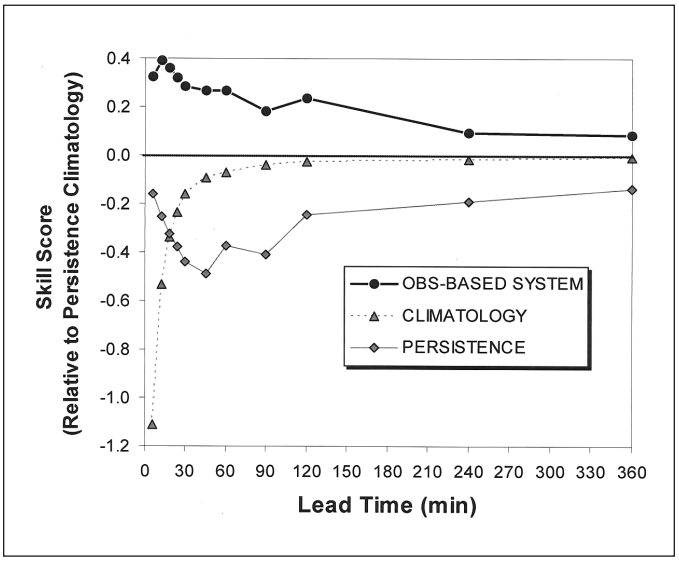


**Figure 10.** Skill score of the observations-based system (black line with circles), climatology (dashed gray line with triangles), and persistence (solid gray line with diamonds) all relative to persistence climatology as a function of lead time. A positive (negative) skill score indicates skill that is better (worse) than persistence climatology.

ing the significance of convective trends in short-term forecasting.

For lead times ≤45 min, radar predictors comprise the top five predictors, after which a greater number of mesonet – then upper-air – predictors are included. By 360-min, most predictors come from either mesonet or upper-air data. Although absolute convergence or relative humidity do not explicitly appear in the top five, it is likely that the criteria incorporated into the mesonet BLPs implicitly accounted for these parameters.

*e. Equation development*

After the best subset of predictors was identified, the most accurate statistical model fit was determined to form the forecast equations. Using a statistical software package (S-PLUS 1999), various statistical model fits (e.g., multiple linear regression (MLR), logistic regression) were tested on the set of best predictors. However, since forecast probabilities can occasionally lie outside the range [0,1] when applying MLR, probabilities were truncated to either 0 or 1, when appropriate. In this study, MLR typically resulted in the lowest MSE.

Once model coefficients were derived using MLR, a working equation for the OKC pixel linking the top predictors for each lead time was formed. Figure 8 shows the explained variance ($R^2$ value) of the developed equations, averaged over all four dependent data set combinations, as a function of lead time. As expected, the explained variance generally decreases with lead time.

Also shown is the relative contribution to the explained variance from each data type. For lead times ≤ 30 min, radar data comprise all the explained variance. The surface mesonet then becomes increasingly significant, contributing 3-5% to the variance for lead times of 90-360 min. The first indication that upper-air data contribute to the forecast system is at 90 min. By 360 min, upper-air data contribute ~4% to the variance, the same magnitude as the mesonet. At this longer lead time, non-radar predictors explain roughly half the explained variance. The figure also shows the contribution of the most recent reflectivity observation at OKC. Note there is a small (< 1%) *independent* contribution of the most recent observation at the 6-min lead time.

## 5. Results: Independent Data

*a. Forecast skill*

Using the developed equations, probabilistic forecasts were generated for each case in each of the independent samples. Mean squared errors were then computed. The MSEs were also calculated by using climatology, persistence, and persistence climatology[3] (PC, a one-predictor equation using the most recent reflectivity observation at OKC). Figure 9 compares the MSE of the obs-based system to each of the three benchmark performance measures as a function of lead time. (The values of MSE in Fig. 9 are an average based on all four independent data sets.) Alternatively, Fig. 10 presents the skill score of the obs-based system relative to PC. For comparison, the skill scores for persistence and climatology are also shown. Because temporal windows were applied in this study that resulted in an artificial increase in number of events with lead time, comparisons of skill score from lead time to lead time must be made with caution.

It is encouraging that the obs-based system is superior (i.e., has a positive relative skill score) to PC for all lead times. Figure 10 shows that the greatest skill is

[3] Persistence climatology is also known as conditional persistence or conditional climatology, as defined in Wilks (1995).

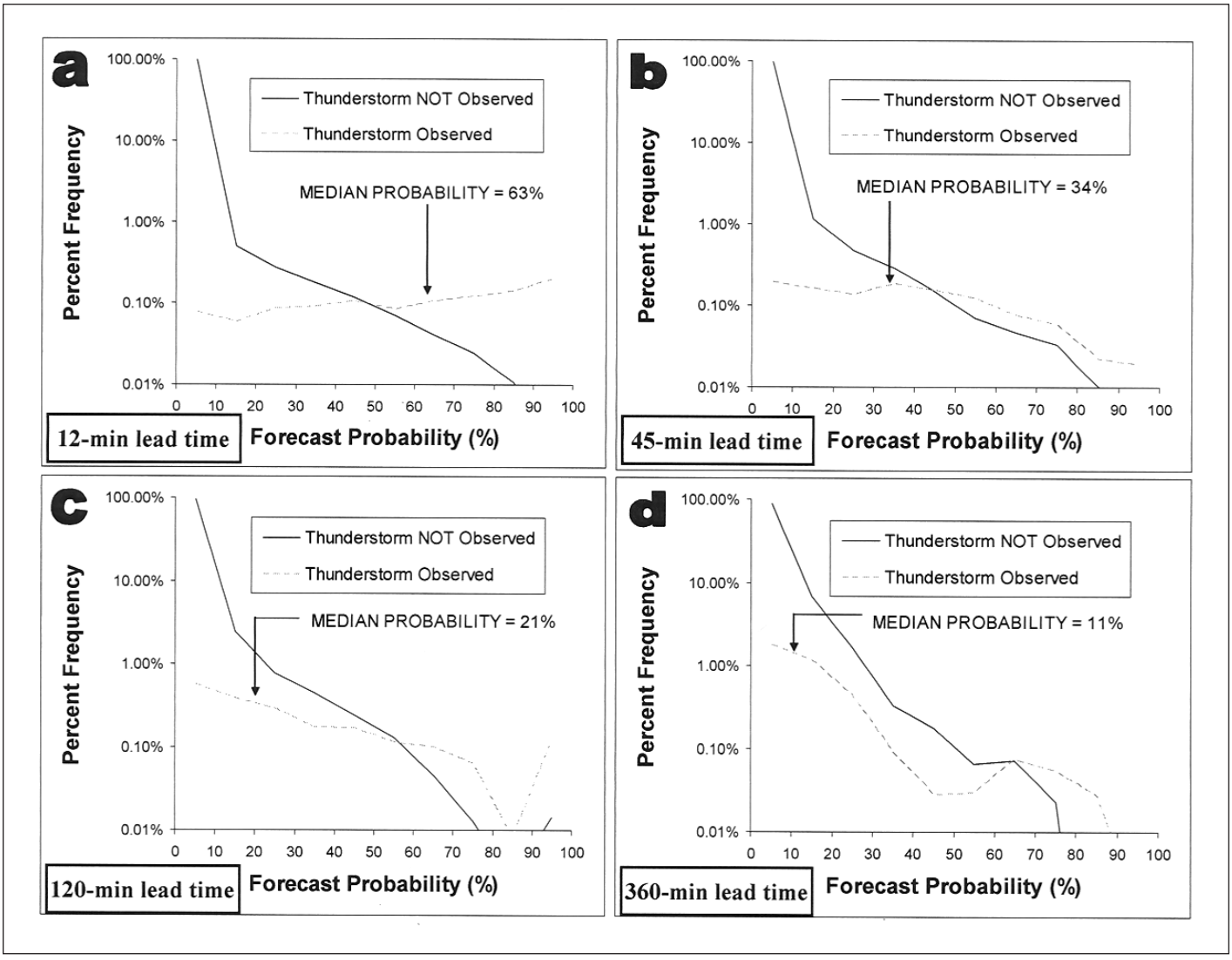


**Figure 11.** Discrimination plots revealing forecast probabilities when convection was observed (dashed lines) and not observed (solid lines) for lead times of: a) 12-min; b) 45-min; c) 120-min; and d) 360-min. Total frequencies sum to 100% on the log axis. The median forecast probability when convection was observed is also labeled for each lead time.

achieved in the shortest lead times tested in this study. A skill of 0.39 is achieved at the 12-min lead time, translating into a 39% reduction in the MSE over PC. Skill gradually decreases with lead time, which is expected considering the system's sole dependence on observations.

When all cases were considered, a paired-difference t-test confirmed that the obs-based forecasts were superior to PC forecasts to a statistically significant degree (in this study, the 99.95% level) *for all lead times*. However, spatial dependence among the forecasts cannot be discounted, which effectively reduces the number of statistically independent cases. The stringent assumption of total spatial dependency was applied, dictating that one-ninth of the cases (i.e., those forecasts from one pixel – the OKC pixel) were retained. A reanalysis of the paired-difference test revealed that the obs-based forecasts remained statistically superior at the 99.95% level through lead times of 360-min[4].

Finally, further examination of Fig. 10 reveals the point in time at which the skill using persistence becomes less than that using climatology when forecasting convection. This transition time is 20 min, testifying to the short-lived nature of convection.

Although MSE is a convenient way to assess probabilistic forecasts, Wilks (1995) emphasizes, MSE is a single – and incomplete – way to evaluate forecast performance. Other scalar attributes of forecast quality, such as forecast bias, discrimination, and reliability, reveal additional information about the joint distribution between forecasts and observations. Two of the aforementioned scalar aspects are now investigated.

[4] The obtained test t-value for the 12-min (360-min) forecasts was 15.7 (5.9), exceeding the critical t-value (using n ∞; 99.95% level) of 3.29.

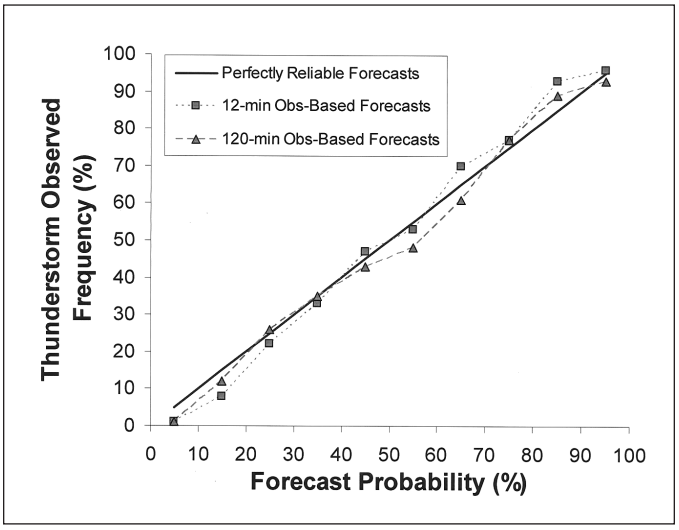


**Figure 12.** Reliability diagram of probabilistic obs-based forecasts for the 12-min (dashed gray line with squares) and 120-min (dashed gray line with triangles) lead times. A set of perfectly reliable forecasts is denoted by the solid black line.

*b. Forecast discrimination*

Figure 11 presents discrimination plots for four lead times from the obs-based system. Shown are distributions of obs-based probabilistic forecasts for the subset of events when: a) convection at OKC was observed (verification probability = 100%), and b) convection at OKC was *not* observed (verification probability = 0%). It is evident from the sold lines in the figure that the most common forecast probability is ~0%, regardless of lead time – a reflection of the infrequent occurrence of convection. Thus, the statistics presented thus far are heavily weighted toward the system's performance during non-convective (i.e., tranquil) conditions. More revealing is how well the system performs during convective situations.

Figure 11 reveals that for the subset of cases where convection did occur (dashed lines), the forecast system overall generated higher probabilities compared to the extremely low value (4%) of using persistence climatology. To indicate this, the median forecast probability when convection was observed is included in the figure. Note that the majority of the forecast probabilities for the 12-min lead time is > 50% (the median probability is 63%). The system's lack of ability to establish all probabilities near 100% when thunderstorms occurred is likely indicative of their short life cycle and highly variable movement. With increasing forecast time, the median probability of convective events expectedly trends lower to 21% at the 120-min lead time, revealing the loss of predictability with time by exclusively using observations.

*c. Forecast reliability*

The principle merit of a forecast system that outputs reliable probabilities allows the user to make decisions with full knowledge of the actual level of risk. A forecast is said to be reliable if its probability matches the event percent frequency over many times the same probability is issued. For example, convection would be expected to be observed 400 out of every 1000 times a reliable 40% probability is issued.

Figure 12 shows the reliability diagram for forecasts from the 12- and 120-min lead times. It is important to reiterate that the forecast sets from which these diagrams were constructed have varying temporal windows and spatial scales (i.e., monitoring areas). Diagrams for other lead times (not shown) confirm that the probabilistic forecasts from this system are generally reliable.

## 6. Summary and Concluding Remarks

Accurate short-term weather forecasts of convection are a critical component to airline operations since convection has a significant impact on the air-traffic flow system. With the availability of several years of high-frequency, mesoscale-resolution weather observations, there is now an opportunity to provide to air-traffic managers a system that can automatically assimilate a multitude of parameters, then reliably and frequently quantify the risk of convection in a timely manner for a multitude of locations via robust, coherent probability fields.

The main results from this study – valid for OKC during May/June – are as follows:

- The observations-based system achieves skill scores, relative to persistence climatology, ranging from 0.09 (360-min lead time) to 0.39 (12-min lead time), with the superiority to persistence climatology statistically significant at the 99.95% level.
- Radar data have the greatest contribution to skill, with an increasing contribution from surface mesonet, then upper-air data, for longer lead times. By 360 min, the forecast equations include predictors from all three data types.
- The most powerful predictor is the percent areal coverage of high reflectivities (typically, a threshold of ≥ 40 dBZ) within an area upstream to OKC.
- Absolute convergence and the climatological departure of relative humidity are the most beneficial predictors from the surface mesonet data.
- The mesonet site that offers the greatest predictability is the one closest west to OKC for a 6-min lead time, ~100 km southwest of OKC for the 30-min lead time, and in extreme southwest Oklahoma for lead times ≥ 60 min.
- The most frequently chosen predictor from the upper-air data is the amount of mid-tropospheric moisture (i.e., 400 mb relative humidity) from the closest radiosonde site to OKC – Norman. Nearby radiosonde sites provide some statistically independent information.

Although this prototype was developed for OKC, a similar process of devising and testing predictors to generate gridded forecasts could be repeated on a national scale. The system's choice of predictors, or its performance, however, may not be representative as shown here because of the current lack of high-resolution observational datasets nationwide.

Conversely, system performance may be enhanced, particularly for the longer lead times, if information on the location/intensity of convection beyond the radar range (i.e., across the Texas and Oklahoma panhandles) as well as upper-level winds upstream of OKC is included. High-quality surface data from the West Texas Mesonet may also increase forecast accuracy. Further improvements in skill for longer lead times could be garnered by incorporating model data into the system (Porter 1995). Forecast equations for an interim period (e.g., 3-9 h) would consist of an optimal blend of model data and observations.

As alluded earlier, the success of this system is directly tied to the robustness of the datasets. Operational data can be noisy, bad, and/or missing. Quality-control algorithms applied to real-time data would complement this forecast system. The quality of the WSR-88D radar data is particularly significant because this data type not only dominates the final forecast equations, but radar data are used as sole verification of the presence of convection. Besides the complexities of identifying non-precipitating echoes or bright-banding, a more serious issue would be beam blockage, a relatively common occurrence in the West, where the mountains interfere with the radar's ability to sample targets. The system would either perform at a degraded level, or not at all if radar coverage were incomplete. Satellite and lightning datasets would then become essential.

## Acknowledgments

The authors wish to thank Art Person and Dipen Kamdar for helping decode radar data, and Stan Benjamin and Eugene Clothiaux for providing RUC model analyses. We would also like to thank the Earth Systems Research Laboratory (formerly the Forecast Systems Laboratory) and the Atmospheric Radiation Measurement Program for access to their profiler and radiosonde data. Finally, we are indebted to J. Paul Dallavalle, David Kristovich, Chris Fiebrich, and Joseph P. Koval for their time and effort placed in reviewing this study. Oklahoma Mesonetwork data are provided courtesy of the Oklahoma Mesonet, a cooperative venture between Oklahoma State University and The University of Oklahoma. This study has been supported under the USWRP/National Science Foundation Grant ATM-9714154 and the U.S. Department of Transportation FAA Grant 2001-G-006.

## Authors

Dr. Joby Hilliker is an assistant professor in the Department of Geology and Astronomy at West Chester University, West Chester, Pennsylvania. Dr. Hilliker received his Ph. D. in 2002 from The Pennsylvania State University, under advisor Dr. J. Michael Fritsch.

Dr. Fritsch is professor emeritus in the Department of Meteorology, and retired from The Pennsylvania State University in 2003.

Dr. George Young is also professor in the Department of Meteorology at The Pennsylvania State University. Dr. Young's research interests include micrometeorology and statistical meteorology, complementing the interests of Drs. Hilliker and Fritsch.

Corresponding Author Information: Joby L. Hilliker, Department of Geology and Astronomy, West Chester University, 223 Boucher Building, West Chester, PA 19383, E-mail: jhilliker@wcupa.edu Phone: (610) 436-2213 Fax: (610) 436-3036.

## References

Benjamin, S. G., D. Devenyi, S. S. Weygandt, K. J. Brundage, J. M. Brown, G. A. Grell, D. Kim,B. E. Schwartz, T. G. Smirnova, T. L. Smith, and G. S. Manikin, 2004: An hourly assimilation-forecast cycle: The RUC. *Mon. Wea. Rev.*, 132, 495-518.

Brock, F. V., K. C. Crawford, R. L. Elliott, G. W. Cuperus, S. J. Stadler, H. L. Johnson, and M. D. Eilts, 1995: The Oklahoma mesonet: A technical overview. *J. Atmos. Oceanic Technol.*, 12, 5-19.

Byers, H. R., and R. R. Braham Jr., 1949: *The Thunderstorm*. U.S. Govt. Printing Office, 187 pp.

Charba, J., 1979: Two to six hour severe local storm probabilities: An operational forecasting system. *Mon. Wea. Rev.*, 107, 268-282.

Corfidi, S. F., J. H. Merritt, and J. M. Fritsch, 1996: Predicting the movement of mesoscale convective complexes. *Wea. Forecasting*, 11, 41-46.

Davies-Jones, R., 1993: Useful formulas for computing divergence, vorticity, and their error from three or more stations. *Mon. Wea. Rev*., 121, 713-725.

Evans, J. E., 2000: Airline operations center usage of FAA terminal weather information products. Preprints, *Ninth Conf. on Aviation, Range, and Aerospace Meteorology*, Orlando, FL, Amer. Meteor. Soc., 76-81.

Fankhauser, J. C., 1964: On the motion and predictability of convective systems. National Severe Storms Project Report 21, 34 pp.

Forman, B. E., M. M. Wolfson, R. G. Hallowell, and M. P. Moore, 1999: Aviation user needs for convective weather forecasts. Preprints, *Eighth Conf. on Aviation, Range, and Aerospace Meteorology*, Dallas, TX, Amer. Meteor. Soc., 526-530.

Garstang, M., and H. J. Cooper, 1981: The role of near surface outflow in maintaining convective activity. *Proc. Nowcasting-I Symp.*, Copenhagen, Denmark, European Space Agency, 161-168.

Germann, U., and I. Zawadski, 2002: Scale-dependence of the predictability of precipitation from continental radar images. Part I: Description of the methodology. *Mon. Wea. Rev.,* 130, 2859-2873.

Glahn, H. R., and D. A. Lowry, 1972: The use of Model Output Statistics (MOS) in objective weather forecasting. *J. Appl. Meteor.*, 11, 1203-1211.

Grover, E. K., 2002: Short-term temperature forecasts with inclusion of radar. M.S. thesis, Dept. of Meteorology, The Pennsylvania State University, University Park, PA, 38 pp.

Hilliker, J. L., and J. M. Fritsch, 1999: An observations-based statistical system for warm-season hourly probabilistic forecasts of low ceiling at the San Francisco International Airport. *J. Appl. Meteor.*, 38, 1692-1705.

_____, 2002: An objective statistical system for short-term probabilistic forecasts of thunderstorms. Ph. D. dissertation, Dept. of Meteorology, The Pennsylvania State University, University Park, PA, 200 pp.

Hughes, K. K., 2004: Probabilistic lightning forecast guidance for aviation. Preprints, *Eleventh Conf. on Aviation, Range, and Aerospace Meteorology*, Hyannis, MA, Amer. Meteor. Soc., CD-ROM, 2.6.

Keith, R., and S. M. Leyton, 2004: An experiment to measure the value of statistical probability forecasts for aerodromes. Preprints, *Eleventh Conf. on Aviation, Range, and Aerospace Meteorology*, Hyannis, MA, Amer. Meteor. Soc., CD-ROM, 9.14.

Kitzmiller, D. H., M. A. R. Lilly, and S. D. Vibert, 2002: The SCAN 0-3 hour rainfall and lightning forecast algorithms. Techniques Development Laboratory, Office of Systems Development, National Weather Service, NOAA, 47 pp.

Kulesa, G., 2002: Weather and Aviation: How does weather affect the safety and operations of airports and aviation, and how does FAA work to manage weather-related effects? *Proc. from the Potential Impacts of Climate Change on Transportation,* Washington, D.C., U.S. Dept. of Transportation, 199-208.

Lee, R. R., 2004: WSR-88D algorithm comparisons of VCP 11 and new VCP 12. Preprints, *20th International Conference on Interactive Information and Processing Systems (IIPS) for Meteorology, Oceanography, and Hydrology*, Seattle, WA, Amer. Meteor. Soc., CD-ROM, 12.7.

Leyton, S. M., and J. M. Fritsch, 2003: Short-term probabilistic forecasts of ceiling and visibility utilizing high-density surface weather observations. *Wea. Forecasting*, 18, 891–902.

_____, and _____, 2004: The impact of high-frequency surface observations on short-term probabilistic forecasts of ceiling and visibility. *J. Appl. Meteor.*, 43**,** 145-156.

MacKeen, P. L., H. E. Brooks, and K. L. Elmore, 1999: Radar reflectivity-derived thunderstorm parameters applied to storm longevity forecasting. *Wea. Forecasting*, 14, 289-295.

Mahoney, J. L., B. G. Brown, and J. Hart, 2000: Statistical verification results for the Collaborative Convective Forecast Product. NOAA Tech. Rep. OAR 457-FSL 6, U.S. Department of Commerce, National Oceanic and Atmospheric Administration, Forecast Systems Laboratory, 30 pp.

Megenhardt, D., C. K. Mueller, N. Rehak, and G. Cunning, 2000: Evaluation of the National Convective Forecast Product. Preprints, *Ninth Conf. on Aviation, Range, and Aerospace Meteorology*, Orlando, FL, Amer. Meteor. Soc., 171-176.

Miller, R. C., 1967: Notes on analysis and severe-storm forecasting procedures of the military Weather Warning Center. AWS Tech. Rep. 200, Headquarters, Air Weather Service, Scott AFB, 94 pp.

Mueller, C., T. Saxen, R. Roberts, and J. Wilson, 2000: Evaluation of the NCAR Thunderstorm Auto-Nowcast System. Preprints, *Ninth Conf. on Aviation, Range, and Aerospace Meteorology*, Orlando, FL, Amer. Meteor. Soc., J40-J45.

_____, _____, _____, _____, T. Betancourt, S. Dettling, N. Oien, and J. Yee, 2003: NCAR Auto-Nowcast System. *Wea. Forecasting*, 18, 545-561.

National Research Council, 2003: Weather forecasting accuracy for Federal Aviation Administration (FAA) traffic flow management: A workshop report. National Academies Press, 68 pp.

National Transportation Safety Board, 1993: Accident briefs. U.S. Govt. Printing Office.

NOAA, cited 2007: National Weather Service NOAA Profiler Network. [Available online at http://www.profiler.noaa.gov/npn].

NOAA/OAR/Earth Systems Research Laboratory, cited 2007: Radiosonde database access. [Available online at http://raob.fsl.noaa.gov].

Neter, J., M. H. Kutner, C. J. Nachtsheim, and W. Wasserman, 1996*: Applied Linear Statistical Models*. 4th ed. Irwin Professional Publishing, 1408 pp.

Porter, C., 1995: Short-term high resolution forecasting of fog, cloud ceiling heights, and visibility with the PSU/NCAR mesoscale model. M.S. thesis, Dept. of Meteorology, The Pennsylvania State University, University Park, PA, 97 pp.

Post, J., J. Bonn, M. Bennett, D. Howell, and D. Knorr, 2002: The use of flight track and convective weather densities for National Airspace System efficiency analysis. *Proc. of the 21st Digital Avionics Systems Conference*, Irvine, CA, 2D4-1 – 2D4-10.

Qualley, W. L., 1997: Impact of weather on and use of weather information by commercial airline operations.

*Workshop on the Social and Economic Impacts of Weather*, Boulder, CO, National Center of Atmospheric Research.

Rhoda, D. A., B. G. Boorman, E. A. Bouchard, M. A. Isaminger, and M. L. Pawlak, 2000: Commercial aircraft encounters with thunderstorms in the Memphis terminal airspace. Preprints, *Ninth Conf. on Aviation, Range, and Aerospace Meteorology*, Orlando, FL, Amer. Meteor. Soc., 37-42.

S-PLUS, 1999: User's guide. Data Analysis Product Division, MathSoft, Seattle, WA, 609 pp.

Sanders, F., and A. J. Garrett, 1975: Application of a convective plume model to prediction of thunderstorms. *Mon. Wea. Rev*., 103, 874-877.

Sankey, D. A., G. J. Kulesa, D. J. Pace, W. L. Fellner, J. E. Sheets, and P. J. Kirchoffer, 2000: Activities of the Federal Aviation Administration's Aviation Weather Research Program. Preprints, *Ninth Conf. on Aviation, Range, and Aerospace Meteorology*, Orlando, FL, Amer. Meteor. Soc., 15-16.

Seseske, S., and J. E. Hart, 2006: Collaborative Convective Forecast Product (CCFP) issuance analysis. Preprints, *12th Conf. on Aviation, Range, and Aerospace Meteorology,* Atlanta, GA, Amer.Meteor. Soc., CD-ROM, J1.3.

Theriault, K.E., M. M. Wolfson, B. E. Forman, R.G. Hallowell, M.P. Moore, and R. J. Johnson, Jr., 2000: FAA Terminal Convective Weather Forecast algorithm assessment. Preprints, *Ninth Conf. on Aviation, Range, and Aerospace Meteorology*, Orlando, FL, Amer. Meteor. Soc., 365-370.

Vislocky, R. L., and J. M. Fritsch, 1997: An automated, observations-based system for short-term prediction of ceiling and visibility. *Wea. Forecasting*, 12, 31-43.

Visual Numerics, Inc., 1997: *Fortran 77 Stat/Library User's Guide Volume 1 and 2.* Visual Numerics, Inc., Houston, TX, 361 pp.

Weather Services Incorporated, cited 2007: An overview of NEXRAD products. [Available online at http://sysu1.wsicorp.com/unidata/intro.html].

Weygandt, S. S., and S. G. Benjamin, 2004: RUC model-based convective probability forecasts. Preprints, *11th Conf. on Aviation, Range, and Aerospace*, Hyannis, MA, Amer. Meteor. Soc., CD-ROM, 5.3.

Wilks, D.S., 1995: *Statistical Methods in the Atmospheric Sciences: An Introduction*. International Geophysics Series, Vol. 59, Academic Press, 464 pp.

Williams, J., 1994: *The USA Today Weather Almanac 1995*. Vintage Books, 390 pp.

Wilson, J. W., N. A. Cook, C. K. Mueller, J. Sun, and M. Dixon, 1998: Nowcasting thunderstorms: A status report. *Bull. Amer. Meteor. Soc.*, 2079-2099.

Zamora, R. J., M. A. Shapiro, and C. A. Doswell III, 1987: The diagnosis of upper tropospheric divergence and ageostrophic wind using profiler wind observations. *Mon. Wea. Rev.*, 115, 871-884.